Antarct. Meteorite Res., **10**, 389–399, 1997

# MINERALOGICAL COMPARISON OF HAMMADAH AL HAMRA 126 WITH SOME UREILITES

Jun CHIKAMI[1], Takashi MIKOUCHI[1], Masamichi MIYAMOTO[1] and Hiroshi TAKEDA[2]

[1]*Mineralogical Institute, Graduate School of Science, University of Tokyo, Hongo, Bunkyo-ku, Tokyo 113*
[2]*Chiba Institute of Technology, 17–1, Tsudanuma 2-chome, Narashino 275*

***Abstract:*** Hammadah al Hamra 126 (HAH 126) is a new ureilite recovered from the Sahara desert in 1995. This meteorite experienced fairly extensive weathering in the desert environment. Olivines in HAH 126 are more intensely reduced than those in other ureilites which have been studied to date. We have obtained a cooling rate of 0.1–0.7°C/hour for the reduction rims of olivines using diffusion calculations. This cooling rate is slightly slower than those for other ureilites. Rims of pigeonite grains in HAH 126 often show high-Ca contents. These Ca-rich materials resemble those which are present at olivine rims in Y-74123 ureilite. This fact suggests that Ca-rich melt was present at grain boundaries (H. OGATa *et al.*; Meteoritics, **25**, 195, 1991).

## 1. Introduction

Ureilites have been defined as pigeonite-olivine achondrites with carbon polymorphs plus metal and troilite in their grain interstices (*e.g.*, MASON, 1962). Because of the discoveries of augite-bearing and orthopyroxene-bearing members from Antarctica (TAKEDA *et al.*, 1989; TAKEDA, 1989), ureilites are now defined as one class of achondrites composed predominantly of olivine and pyroxene with carbonaceous materials and metal at grain interstices. They preserve oxygen isotope signature of chondritic materials (CLAYTON and MAYEDA, 1988) and high noble gas contents (BEGEMANN and OTT, 1983), although they exhibit coarse-grained achondritic textures similar to terrestrial ultramafic rocks. To date, 39 ureilites including Japanese, United States and European finds have been recovered from Antarctica and 13 ureilites have been recovered outside Antarctica. Antarctic ureilites have given us a wealth of information on the genesis of ureilites, because Antarctic ureilites show a wider range in chemical composition than non-Antarctic ureilites. Despite the presence of 52 recovered ureilites, satisfactory models for ureilite formation have not been proposed because it is very difficult to explain both the chondritic and achondritic features of ureilites.

Hammadah al Hamra 126 (HAH 126) is a new ureilite recovered from the Sahara desert. SEXTON *et al.* (1996) suggested on the basis of the compositions of olivine cores and the oxygen and carbon isotopic compositions of HAH 126 that this meteorite is a Group 1 ureilite in the scheme of CLAYTON and MAYEDA (1988). They also suggested that HAH 126 is closely related to the Y-74123 ureilite which has a simi-

lar oxygen isotopic composition, although there are some differences between these two meteorites such as shock stage and degree of metal exsolution. We compared HAH 126 especially with Y-74123.

Y-74123 is an olivine-rich, mediumly shocked ureilite and only 3 vol% pigeonite has been detected (TAKEDA, 1987; GOODRICH, 1992). It contains more abundant interstitial materials than other studied ureilites (OGATA *et al.*, 1991). Bulk chemical composition of the interstitial materials in Y-74123 is pyroxene-like and has high CaO and $Al_2O_3$ contents.

We also compared HAH 126 with ALH82106 that is the most Mg-rich ureilite. BERKLEY *et al.* (1985) indicated that olivine of the ALH82106 shows complete reduction at the rim. CHIKAMI *et al.* (1996) and SEXTON *et al.* (1996) found that reduction of olivine in HAH 126 is more extensive than those in other ureilites. We performed mineralogical analysis of HAH 126, focusing on olivine reduction and interstitial material, and compared it with other known ureilites, especially Y-74123 and ALH82106.

Since the major topics of this study are concerned with events after the major formation processes of ureilites, we will not discuss about their formation models recently proposed by WARREN and KALLEMEYN (1992), SCOTT *et al.* (1993) and TAKEDA (1989).

## 2. Sample and Experimental Techniques

HAH 126 was found in 1995 during a collection trip to the Hammadah al Hamra region of Libya (28°28′N, 12°56′E) (BISCHOFF and GEIGER, 1995). A single stone of 1988 g was recovered. HAH 126 is fairly weathered due to severe environments in the desert. The degree of shock metamorphism was obtained by using the shock classification system for olivine (STÖFFLER *et al.*, 1991). A weathering degree of HAH 126 was also estimated from the degree of oxidation observed in a thin section (JULL *et al.*, 1990; WLOTZKA, 1993). HAH 126 shows the shock stage of S3 and the weathering degree of W3 (WEBER and BISCHOFF, 1996).

The thin section of HAH 126 that we studied was generously prepared at National Institute of Polar Research (NIPR). The thin sections of Y-74123 and ALH82106 were supplied by the NIPR. Petrography of the thin sections (HAH 126 and Y-74123) has been examined by optical and scanning electron microscopy (JEOL JXA-840A) at Mineralogical Institute, University of Tokyo. The electron microscopy was completed in the Electron Microbeam Analysis Facility of the Mineralogical Institute, University of Tokyo. Quantitative analyses of minerals were performed using electron probe microanalyzers (JEOL EPMA JCXA-733 at the Ocean Research Institute, University of Tokyo and JEOL EPMA JCXA-733mk II at the Geological Institute, University of Tokyo). Thirteen elements (Si, Ti, Al, Fe, Mn, Mg, Ca, Na, K, Cr, V, Ni and P) were measured. Accelerating voltage was 15 kV and beam current was 12 nA. Elemental distribution maps were obtained using the electron probe microanalyzer (JEOL JXA-8900L) at the Geological Institute, University of Tokyo. Seven elements (Si, Mg, Ca, Fe, Cr, Al and Ni) were measured. Accelerating voltage was 15 kV and beam current was 120 nA.

We have estimated the cooling rate of HAH 126 olivine using the Fig. 5 of

MIYAMOTO *et al.* (1985). The reverse zoning (Mg enrichment) at the grain boundary of ureilite olivines is generally thought to be formed as a result of reduction by the carbon matrix (BERKLEY *et al.*, 1976). In the diagram, cooling rates to produce the zoning profile have been estimated by numerically solving the diffusion equation (MIYAMOTO *et al.*, 1985). It was assumed that iron atomic diffusion produces the zoning profile (BERKLEY *et al.*, 1976), although the reduction mechanism may be more complex. The diffusion coefficient parallel to the *c* axis of olivine was employed for calculation (BUENING and BUSECK, 1973). The calculation assumes a linear cooling from initial temperature, T, to 800°C to fit calculated profiles to the observed profile. The initial temperature is estimated from the chemical compositions of coexisting pyroxenes using the pyroxene geothermometer of LINDSLEY and ANDERSON (1983). We used 1200–1300°C as the initial temperature for the olivine reduction in HAH 126, because the temperatures for coexisting pyroxene pairs in ureilites studied to date, are 1200–1300°C (CHIKAMI *et al.*, 1995).

## 3. Results

### *3.1. Mineralogy of Hammadah al Hamra 126*

The major mineral assemblage of HAH 126 is olivine and pigeonite (Fig. 1). Grain sizes of olivine range from 0.4 mm to 1.9 mm in diameter and those of pigeonite range from 0.2 mm to 0.9 mm. The pigeonite grains are elongated (Figs. 1, 2). Some olivine grains are surrounded by pigeonite grains. Many cracks are observed in the interior of most olivine grains (Fig. 1). The outer shapes of olivine grains are irregular due to intense reduction at their rims. Intensely reduced portion, which was orig-

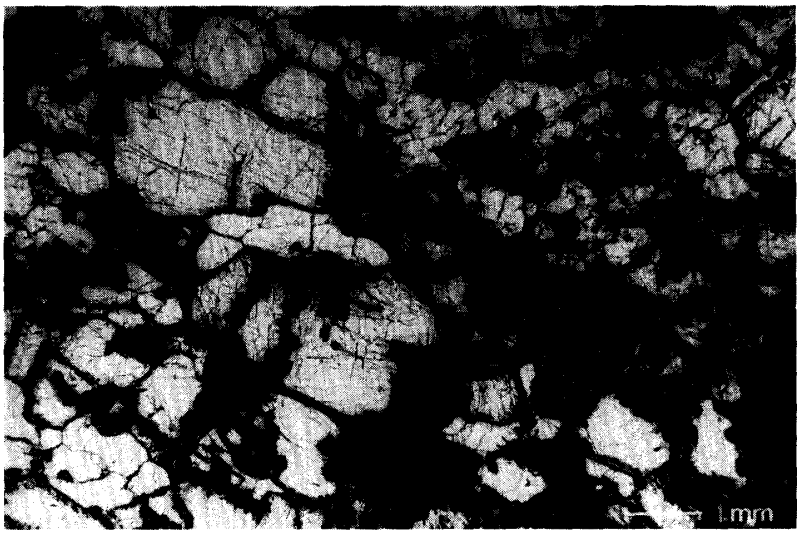


*Fig. 1. Photomicrograph of HAH 126. Width is 10.6 mm. Crystals with many cracks are olivine and elongated crystals are pigeonite. The grain edges of olivine are irregular due to intense reduction. Large dark portions are intensely reduced portions which were originally olivine. Black portions at grain boundaries are carbon matrix.*

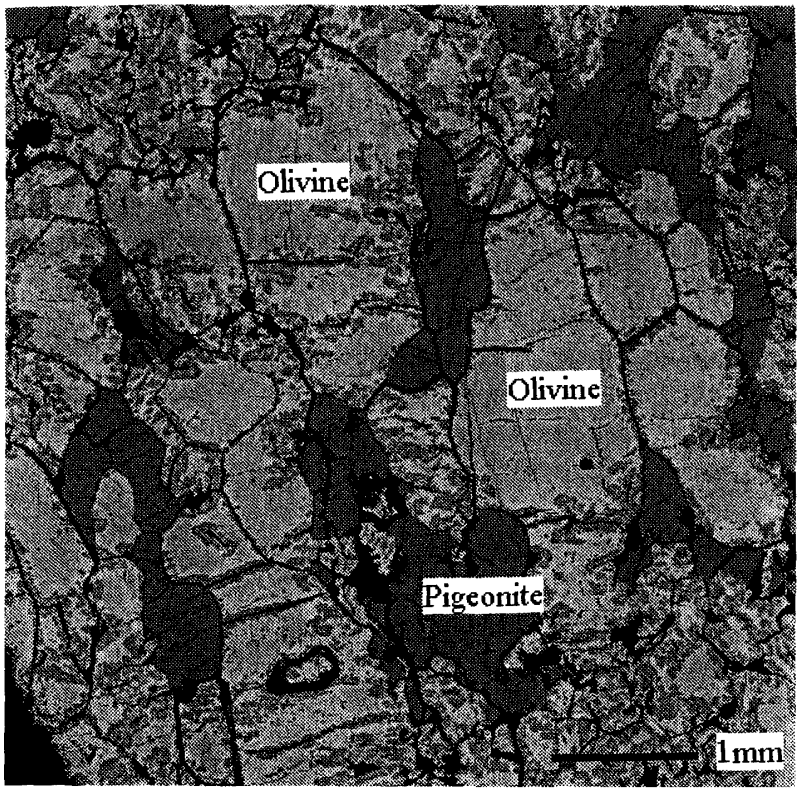


*Fig. 2. Mg elemental distribution map of HAH 126. The areas of high Mg concentration (the bright grayish portion) are olivine grains. Olivine crystals show reduction rims (from bright gray to white). The darker grayish portions in olivine were olivine before the intense reduction. The dark grayish portions are pigeonite grains.*

*Table 1. Chemical compsition (wt%) of olivine, pigeonite and interstitial materials in HAH 126 ureilite.*

| | Core | | Rim materials | |
|---|---|---|---|---|
| | olivine | pigeonite | Ca-poor | Ca-rich |
| $SiO_2$ | 38.8 | 55.1 | 54.9 | 52.8 |
| $Al_2O_3$ | 0.01 | 0.33 | 1.00 | 1.66 |
| $TiO_2$ | 0.02 | 0.04 | 0.12 | 0.65 |
| FeO | 18.2 | 11.0 | 8.42 | 6.61 |
| MnO | 0.40 | 0.43 | 0.44 | 0.22 |
| MgO | 40.6 | 27.4 | 27.5 | 16.8 |
| CaO | 0.39 | 3.99 | 7.03 | 20.5 |
| $Na_2O$ | 0.01 | 0.04 | 0.04 | 0.35 |
| $K_2O$ | – | – | – | 0.01 |
| $Cr_2O_3$ | 0.59 | 1.09 | 1.14 | 0.27 |
| $V_2O_3$ | 0.02 | 0.03 | 0.02 | 0.07 |
| NiO | 0.02 | 0.02 | 0.07 | 0.05 |
| Total | 99.06 | 99.47 | 100.68 | 99.99 |

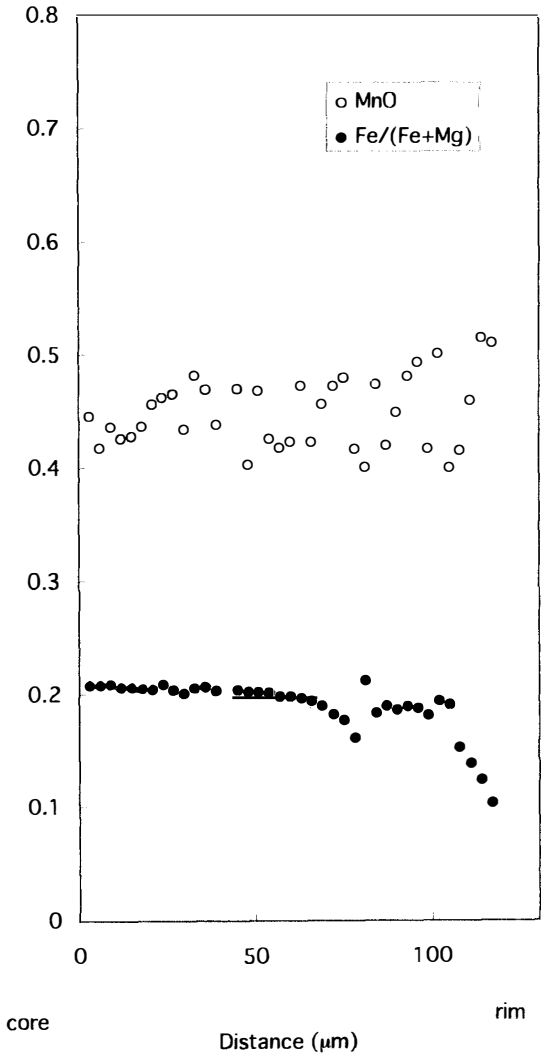


*Fig. 3. An example of chemical zoning of olivine in the HAH 126 ureilite. Solid circles: Fa component (=atomic Fe/(Fe+Mg)); open circles: MnO content (wt%). Atomic Fe/(Fe+Mg) and wt% versus a distance in microns from core to rim in olivine are plotted for an olivine crystal.*

inally olivine before it suffered from reduction, are dark-brown in color in transmitted light in the optical microscope. Olivine cores are uniform in composition ($Fa_{20}$) (Table 1). The rims *ca.* 70–100 $\mu$m from the grain boundaries are reduced by carbon and show more magnesian compositions than the cores (brighter colored portion in Fig. 2, Fig. 3). Olivine crystals also show reduction along interior cracks in the crystal. The cores of pigeonite grains have homogeneous chemical compositions of $Ca_8Mg_{75}Fe_{17}$ (Table 1). Pigeonite crystals exhibit less reduction due to much slower atomic diffusion rate of Mg-Fe than olivine. Interstices of mafic silicate grains are filled with Fe-rich metal and carbonaceous matrix. Modal abundances of minerals obtained by elemental distribution maps are: olivine 56 vol%, pigeonite 26 vol%, and

others 18 vol%. The pyroxene/(pyroxene+olivine) volume ratio of *ca.* 0.3 is typical of other ureilites.

### *3.2. Ca-rich materials of HAH 126*

We observed Ca-rich material rimming several pigeonite grains. These rims are located between pigeonite and carbon matrix, and others are between pigeonite and olivine (Figs. 4a, b). The Ca-rich material is nearly identical to pyroxene composition and is $Ca_{11}Mg_{81}Fe_{8}$ - $Ca_{41}Mg_{48}Fe_{11}$ (Fig. 5). $Al_2O_3$ content of the Ca-rich rims is 1.0–1.6 wt% and $Cr_2O_3$ content is 0.3–1.1 wt%.

### *3.3. Cooling rate of olivine*

The core composition of olivine is fairly uniform ($Fa_{20}$), while Mg contents (forsterite) show enrichment at rims (~70–100 $\mu$m) ($Fa_3$-$Fa_5$) as stated before. The Mn content of olivine slightly increases (MnO: 0.4~0.5 wt%) as the Fa content decreases. We have obtained the chemical zoning profile of olivine in HAH 126 by line analysis (Fig. 3). Using the Fig. 5 of MIYAMOTO *et al.* (1985), the cooling rate of 0.1–0.7°C/hour gives the best fit for the observed zoning profiles of olivine reduction rims in HAH 126. This cooling rate is slightly slower than other ureilites (0.5–6.0°C/hour) which we have analyzed (CHIKAMI *et al.*, 1996).

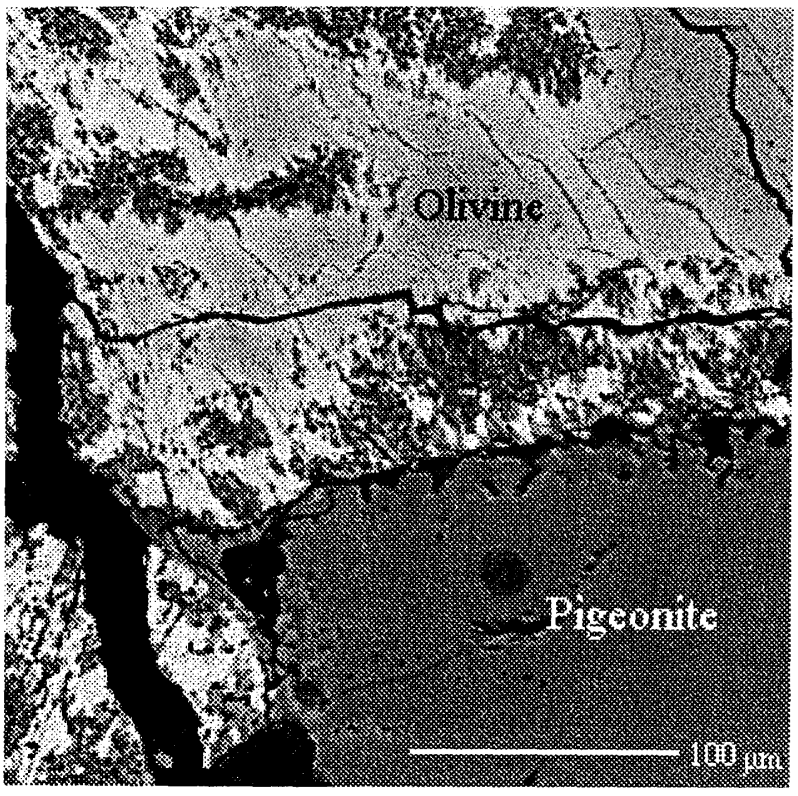


*Fig. 4a. Mg elemental distribution map of HAH 126. The areas of high Mg concentration (the bright grayish portion) are olivine. Note intense reduction at a rim and interior crack of the olivine (white portion). The dark grayish portion is a pigeonite grain.*

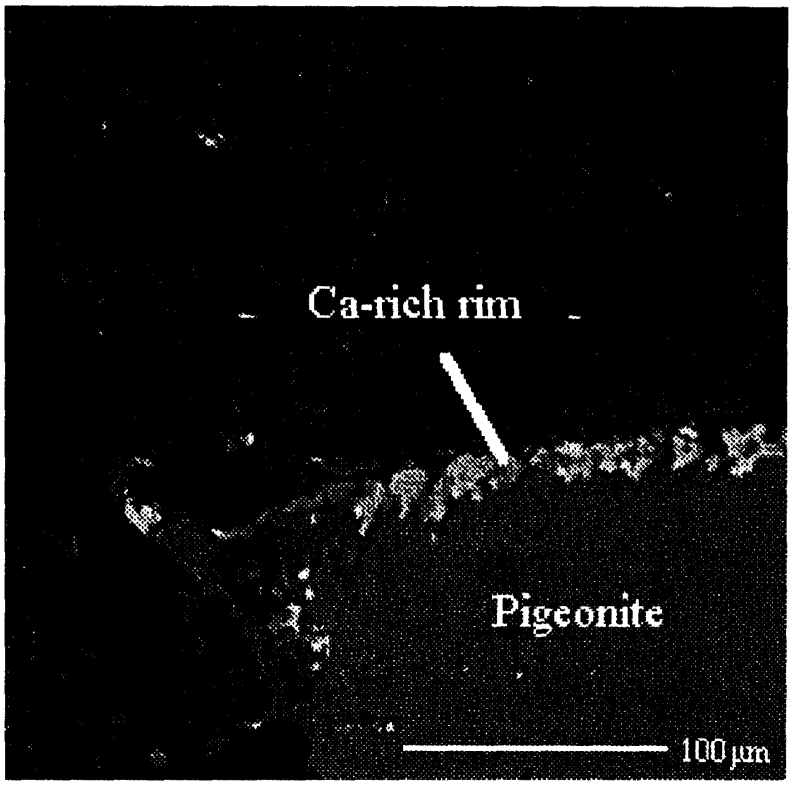


*Fig. 4b. Ca elemental distribution map of HAH 126. This area is the same portion and same scale of Fig. 4a. The white portion around the pigeonite grain indicates high Ca concentration and is a Ca-rich rim.*

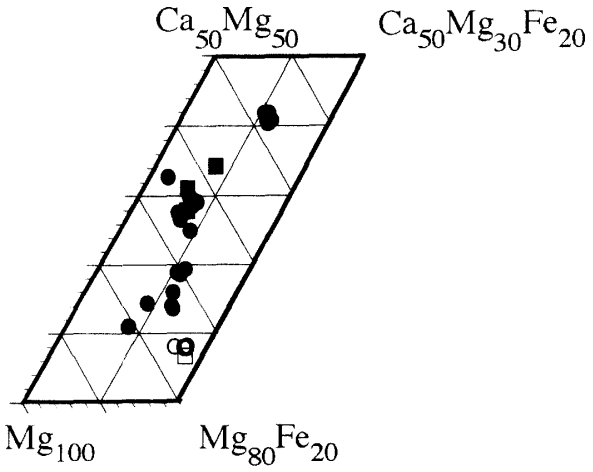


*Fig. 5. The compositions of pigeonites and Ca-rich rims in HAH 126 and Y-74123 plotted in the pyroxene quadrilateral. Open circles: pigeonite (core) in HAH 126; solid circles: Ca-rich rims in HAH 126; open squares: pigeonite (core) in Y-74123 (OGATA et al., 1991); solid squares: Ca-rich rims in Y-74123 (OGATA et al., 1991).*

## 4. Discussion

BERKLEY *et al.* (1985) indicated that olivine of the ALH82106 ureilite shows complete reduction at the rim of most grains. We compared olivine of HAH 126 with that of ALH82106 focusing on reduction, because olivine of HAH 126 also shows intense reduction. BERKLEY *et al.* (1985) also indicated that olivine core and pigeonite core of ALH82106 have mg = 95 (mg: atomic%, Mg/(Mg + Fe)) and that olivine in ALH82106 shows complete reduction to 100% Fo at rims of most grains, because ALH82106 crystallized from a high-T and highly reduced magma. We analyzed ALH82106 in order to compare it with HAH 126, found that olivine crystals of ALH82106 show Mg enrichment at rims, and estimated a cooling rate of 1.8°C/hour. The range of ALH82106 reduction (~20 $\mu$m) is smaller than that of HAH 126 (~70–100 $\mu$m) although the Fa content of ALH82106 olivine core ($Fa_3$) is much more Mg-rich than that of HAH 126. CHIKAMI *et al.* (1996) suggested that cooling rates deduced from olivine reduction rims in ureilites are similar although the Fa components of olivine are variable in ureilites. The Fa contents of olivine core represent the degree of reduction, that is, olivine core composition reflect the oxidation state of crystallization and annealing stage from a melt produced from the source material. On the other hand, the formation of reduction rims depends on the degree of cooling (final stage cooling rate) when parts of the hot parent body were excavated by the break up of the body or impact into the body.

We performed the estimation of the cooling rates from the chemical zoning of olivines for 8 ureilites including HAH 126 (CHIKAMI *et al.*, 1996). These results also support that olivines of HAH 126 are more reduced than other ureilites and that the final stage cooling rate for the HAH 126 olivine is slightly slower than other ureilites.

SEXTON *et al.* (1996) indicated that HAH 126 is most closely related to Y-74123 because they have almost identical isotopic compositions. Y-74123 contains abundant interstitial materials (OGATA *et al.*, 1991). We compared HAH 126 with Y-74123 focusing on interstitial materials. The Fa content of Y-74123 ($Fa_{19}$) is also almost identical to that in HAH 126 ($Fa_{20}$). However, the over all abundance of pigeonite in Y-74123 (3 vol%) is much smaller than that in HAH 126 (26 vol%). The Ca content of pigeonite in Y-74123 ($Ca_6Mg_{76}Fe_{18}$) is similar to that in HAH 126 ($Ca_8Mg_{75}Fe_{17}$). The Fe content of pigeonite in Y-74123 is similar to that in HAH 126. Olivine crystals of Y-74123 are often coated by thin "pigeonitic" rims (3–20 $\mu$m) of pyroxene compositions (OGATA *et al.*, 1987). We found that the pigeonite of HAH 126 has augite-like rims and that olivines do not contain a Ca-rich rim. The composition of Ca-rich rims around the Y-74123 pigeonite ($Ca_{9\text{-}30}Mg_{60\text{-}77}Fe_{8\text{-}13}$) is similar to that in HAH 126 ($Ca_{11\text{-}41}Mg_{81\text{-}48}Fe_{8\text{-}11}$). OGATA *et al.* (1987) reported that the enrichment of Ca and Al is observed at the Y-74123 olivine rims and that the Al-rich portions contain 6–7 wt% $Al_2O_3$. The augite-like rims in HAH 126 contain less $Al_2O_3$ content (1.0 wt%) than the Ca-Al-rich rims in Y-74123. Except for $Al_2O_3$ content, augite-like rims of pigeonite in HAH 126 resemble those of Y-74123 in chemical composition. OGATA *et al.* (1987) also indicated that ALH78019 and Y-82100 contain similar "pigeonitic" rim materials. The Ca-rich rim materials of Y-82100 are present at pyroxene-pyroxene boundaries.

Reduction rims of olivine in ureilites were produced by carbon veins during the cooling period after the break-up of the parent body. They are generally composed of enstatite with low Fe and Ca contents. MORI and TAKEDA (1983) reported the presence of low-Ca pyroxene in the vicinity of the rim of an ALH77257 ureilite olivine grain. There is a possibility that the interstitial materials may have been reduced by the carbon veins, as happened with olivine grains. There are differences in the texture between the interstitial materials and the reduction rims, when examined by TEM (OGATA *et al.*, 1991). The large sizes of the high-Ca pyroxene in the Y-74123 interstitial materials, and absence of any other phases nucleated in it, are in contrast to cloudy pigeonite of the Y-790981 ureilite, in which many phases were produced by shock melting on a very small scale (OGATA *et al.*, 1991). Moreover, this view is also supported by the fact that glassy materials produced by shock melting in Y-790981 cut the rim materials (OGATA *et al.*, 1991). These facts would suggest that the Ca-rich rim materials in Y-74123 and HAH 126 could not have formed by a reduction reaction and that they had already solidified when the break-up of the ureilite parent body.

GOODRICH (1986) suggested that the interstitial material represents trapped primary liquid during the cumulate process. If the model of GOODRICH (1986) is correct, they should have higher CaO contents at olivine-olivine grain boundaries than at olivine-pyroxene grain boundaries, since calcium are incorporated into pyroxene and not into olivine. In Y-74123, CaO contents of Ca-rich interstitial materials at olivine-pyroxene boundaries are higher than at olivine-olivine boundaries (OGATA *et al.*, 1991). NAKAMURA (1994) performed shock experiments for CV3 chondrites. He observed that Ca-Si-rich glassy grains which has composition close to augite (CaO 23 wt%, $SiO_2$ 49%) were produced by shock. This composition resembles those of Ca-rich rims in Y-74123 (CaO 14–15 wt%, $SiO_2$ 50–54%) and HAH 126 (CaO 7–20 wt%, $SiO_2$ 52–54%). From these facts, we agree with a view that some residual liquids of high Ca concentration were present at one time along grain boundaries and they were mixed with later liquid produced by partly melting of olivines and pigeonites produced by a heating event, probably by impacts, before the parent body break up.

## 5. Conclusions

(1) HAH 126 mainly consists of olivine and pigeonite. This mineral assemblage and mineral chemistry of HAH 126 are common in ureilites.

(2) Olivine crystals in HAH 126 were intensely reduced and have characteristics of wide reduction rims. The cooling rate (0.1–0.7°C/hour) deduced from the reduction rim of olivine is slightly slower than other ureilites, although this cooling rate is within the range of other ureilites.

(3) Rims of several pigeonite grains in HAH 126 show a high Ca content as reported in the Y-74123 and ALH78019 ureilites which also contain Ca-rich rims.

## Acknowledgments

We are indebted to the National Institute of Polar Research for preparation of a thin section of Hammadah al Hamra 126 and providing us with other Antarctic ure-

ilite samples. Hammadah al Hamra 126 is from the sample collection of the Planetary Materials Database of University of Tokyo. We thank Mr. O. TACHIKAWA at Mineralogical Institute, and Mr. H. YOSHIDA at Geological Institute, University of Tokyo for their technical assistance. We thank Dr. P. H. WARREN for helpful discussion and Drs. T. McCOY and Y. IKEDA for constructive reviews. This work was supported by JSPS Research Fellowship for Young Scientists (J. C.).

## References

BEGEMANN, F. and OTT, U. (1983): Comment on "The nature and origin of ureilites" by J. L. BERKLEY *et al.* Geochim. Cosmochim. Acta, **47**, 975–977.

BERKLEY, J. L., BROWN, H. G. IV, KEIL, K., CARTER, N. L., MERCIER, J-C.C. and HUSS, G. (1976): The Kenna ureilite: An ultramafic rock with evidence for igneous, metamorphic and shock origin. Geochim. Cosmochim. Acta, **40**, 1429–1437.

BERKLEY, J. L., GOODRICH, C. A. and KEIL, K. (1985): The unique ureilite, ALH82106-82130: Evidence for progressive reduction during ureilite magmatic differentiation. Meteoritics, **20**, 607–608.

BISCHOFF, A. and GEIGER, T. (1995): Meteorites form the Sahara: Find locations, shock classification, degree of weathering and paring. Meteoritics, **30**, 113–122.

BUENING, D. K. and BUSECK, P. R. (1973): Fe-Mg lattice diffusion in olivine. J. Geophys. Res., **78**, 6852–6862.

CHIKAMI, J., MIKOUCHI, T., MIYAMOTO, M. and TAKEDA, H. (1995): Equilibration temperature of Lewis Cliff 88774 and other ureilites. Meteoritics, **30**, 498.

CHIKAMI, J., MIKOUCHI, T., MIYAMOTO, M. and TAKEDA, H. (1996): Mineralogy and cooling history of FRO90054 compared to other ureilites. Lunar and Planetary Science XXVII. Houston, Lunar Planet. Inst., 221–222.

CLAYTON, R. N. and MAYEDA, T. K. (1988): Formation of ureilites by nebular processes. Geochim. Cosmochim. Acta, **52**, 1313–1318.

GOODRICH, C. A. (1986): Trapped primary silicate liquid in ureilites. Lunar and Planetary Science XVII. Houston, Lunar Planet. Inst., 273–274.

GOODRICH, C. A. (1992): Ureilite: A critical review. Meteoritics, **27**, 327–352.

JULL, A. J. T., WLOTZKA, F., PALME, H. and DONAHUE, D. J. (1990): Distribution of terrestrial age and petrologic type of meteorites from western Libya. Geochim. Cosmochim. Acta, **54**, 2895–2898.

LINDSLEY, D. H. and ANDERSON, D. J. (1983): A two-pyroxene thermometer. Proc. Lunar Planet. Sci. Conf., 13th, Pt. 2, A887–906 (J. Geophys. Res., **87** Suppl.)

MASON, B (1962): Meteorites. J. Wiley, New York, 274p.

MIYAMOTO, M., TAKEDA, H. and TOYODA, H. (1985): Cooling history of some Antarctic ureilites. Proc. Lunar Planet. Sci. Conf., 16th, Pt. 1, D116–122 (J. Geophys. Res., **90**, Suppl.)

MORI, H. and TAKEDA, H. (1983): Deformation of olivine in the Antarctic ureilites, Allan Hills 77257 and 78262. Lunar and Planetary Science XIV. Houston, Lunar Planet. Inst., 519–520.

NAKAMURA, T. (1994): Shock metamorphism of carbonaceous chondrites: Mineralogical and textural diversity of experimentally shocked Allende CV3 and Leoville CV3 chondrites. Doctor Thesis, Mineralogical Institute, University of Tokyo.

OGATA, H., TAKEDA, H. and ISHII, T. (1987): Interstitial Ca-rich silicate materials in the Yamato ureilites with reference to their origin. Lunar and Planetary Science XVIII. Houston, Lunar Planet. Inst., 738–739.

OGATA, H., MORI, H. and TAKEDA, H. (1991): Mineralogy of interstitial rim materials of the Y74123 and Y790981 ureilites and their origin. Meteoritics, **26**, 195–201.

SCOTT, E. R. D., TAYLOR, G. J. and KEIL, K. (1993): Origin of ureilite meteorites and implications for planetary accretion. Geophys. Res. Lett., **20**, 415–418.

SEXTON, A., FRANCHI, I. A. and PILLINGER, C. T. (1996): Hammadah al Hamra 126–a new Saharan ureilite. Lunar and Planetary Science XXVII. Houston, Lunar Planet. Inst., 1173–1174.

STÖFFLER D., KEIL, K. and SCOTT, E. R. D. (1991): Shock metamorphism of ordinary chondrites. Geochim.

Cosmochim. Acta, **55**, 3845–3867.

TAKEDA, H. (1987): Mineralogy of Antarctic ureilites and a working hypothesis for their origin and evolution. Earth Planet. Sci. Lett., **81**, 358–370.

TAKEDA, H. (1989): Mineralogy of coexisting pyroxenes in magnesian ureilites and their formation process. Earth Planet. Sci. Lett., **93**, 181–194.

TAKEDA, H., MORI, H. and OGATA, H. (1989): Mineralogy of augite-bearing ureilites and the origin of their chemical trends. Meteoritics, **24**, 73–81.

WARREN, P. H. and KALLEMEYN, G. W. (1992): Explosive volcanism and the graphite-oxygen fugacity buffer on the parent asteroid(s) of the ureilite meteorites. Icarus, **100**, 110–126.

WEBER, D. and BISCHOFF, A. (1996): New meteorite finds from the Libyan Sahara. Lunar and Planetary Science XXVII. Houston, Lunar Planet. Inst., 1393–1394.

WLOTZKA, F. (1993): A weathering scale for the ordinary chondrites. Meteoritics, **28**, 460.

*(Received August 30, 1996; Revised manuscript accepted November 11, 1996)*